International Journal of Nanoelectronics and Materials
Volume 15 (Special Issue) December 2022 [351-358]

Analysis of Power Distribution in Mach Zehnder Interferometer Polymer-based Waveguide for Sensing Applications

Mohd. Azarulsani Md. Azidin[1,2,*], Nurjuliana Juhari[1,2], Arif Mawardi Ismail[1], and Norhayati Sabani[1,2]

[1]Micro System Technology, Centre of Excellence (MiCTEC), Universiti Malaysia Perlis, 02600 Arau, Perlis, Malaysia
[2]Faculty of Electronic Engineering & Technology, Universiti Malaysia Perlis, 02600 Arau, Perlis, Malaysia

ABSTRACT

Two Mach Zehnder Interferometer (MZI) polymer-based waveguide designs namely MZI symmetrical and MZI asymmetrical structures were simulated and analyzed using Optiwave OptiBPM10. The two designs with device size of 4000µm x 300µm exhibit clear optical propagation path when light is simulated through them as well as displaying single mode profile. Highest output power was obtained by the MZI symmetrical design at 0.90 a.u, which suggests better waveguide design for sensing applications.

Keywords: Mach-Zehnder Interferometer, waveguide, optical power distribution, optical sensor

1. INTRODUCTION

Interferometric sensors especially Mach Zehnder Interferometer (MZI) based sensors have already been developed and applied since the early 1990s [1]. From there, it evolved into much sophisticated sensors that is used for many applications. One example is a researcher who created a cost effective MZI liquid refractive index sensor based on a conventional polymer strip waveguide that can achieve high sensitivity with having different reference arm lengths [2]. Other typical applications are high sensitivity temperature sensor [3], heavy metal sensor [4], volatile organic compounds detector [5], displacement sensor [6], thermal-optical switch [7], surface sensor [8] and many more.

MZI was developed by Ludwig Mach and Ludwig Zehnder where it uses two separate beam splitters to split, recombine the light beams and has two outputs. The optical path lengths in the two arms maybe identical or it might differ from each other. The optical power distribution of the two outputs depends on the precise difference in optical arms' length and wavelength [9].

This work reports on the analysis of power distribution of MZI polymer-based waveguide of different designs and shapes. These designs use polymer SU8 as core, poly(methyl methacrylate) (PMMA) as cladding and silicon as substrate. The main motivation for this research is to investigate whether the two waveguide designs will have proper optical beam propagation and to check for highest optical power output obtained from them.

* azarulsani@unimap.edu.my

2. PRINCIPAL THEORY

Our MZI consists of two Y-branches, which are connected by two waveguides of different length, L_1 (sensing arm) and L_2 (reference arm), and different propagation constants, $\gamma_1 = \alpha_1 + i\beta_1$ and $\gamma_2 = \alpha_2 + i\beta_2$. Let I_i and I_o be the input and output intensity of the MZI respectively, and their corresponding electric fields be denoted by E_i and E_o. At the input Y-branch, the light intensity is split equally, and the electric fields, E_{i1} and E_{i2}, in the two waveguides right after the input Y-branch read [10]:

$$E_{i1} = E_{i2} = \frac{E_i}{\sqrt{2}} \tag{1}$$

At the ends of the waveguides, the electric fields read:

$$E_{o1} = E_{i1}e^{-\gamma_1 L_1} = E_{i1}e^{-i\beta_1 L_1 - \alpha_1 L_1} = \frac{E_i}{\sqrt{2}}e^{-i\beta_1 L_1 - \alpha_1 L_1} \tag{2}$$

$$E_{o2} = E_{i2}e^{-\gamma_2 L_2} = E_{i2}e^{-i\beta_2 L_2 - \alpha_2 L_2} = \frac{E_i}{\sqrt{2}}e^{-i\beta_2 L_2 - \alpha_2 L_2} \tag{3}$$

At the combiner side, the output of the Y-branch is as follows:

$$E_o = \frac{E_{o1} + E_{o2}}{\sqrt{2}} = \frac{E_i}{2}(e^{-i\beta_1 L_1 - \alpha_1 L_1} + e^{-i\beta_2 L_2 - \alpha_2 L_2}) \tag{4}$$

And $I_o = |E_o|^2$,

$$I_o = \frac{I_i}{4}\left|e^{-i\beta_1 L_1 - \alpha_1 L_1} + e^{-i\beta_2 L_2 - \alpha_2 L_2}\right|^2 \tag{5}$$

In lossless waveguides $\alpha_1 = \alpha_2 = 0$, $\beta_1 = \beta_2 = \beta$ and $\Delta L = L2 - L1$, then Equation 5 will now be:

$$I_o = \frac{I_i}{2}[1 + \cos(\beta \Delta L)] \tag{6}$$

Equation 6 exists only in ideal condition whereas Equation 5 occurs in real condition where there will be a loss in the waveguides when light propagates through them [11].

2.1 Simulation Setup

This research is performed by simulating optical beam propagation through a waveguide in various sizes using an optical beam propagation simulation software called Optiwave OptiBPM10 operating at single mode transmission. There are two main waveguide designs that were under analysis: MZI symmetrical and MZI asymmetrical structures. A rectangular waveguide width of 4μm and a device size of 4000μm x 300μm is used in the designs.

The designs were running on the following parameters shown in Table 1 and Table 2.

Table 1 Materials, refractive indices and thickness parameters

Materials	Refractive Index	Thickness (μm)
Cladding: PMMA	1.48	8
Core: SU8	1.60	4

Table 2 2D simulation parameters

Parameters	Values/Method
Polarization	TE & TM
Wavelength (nm)	1550
BPM Solver	Paraxial
Engine	Finite Difference
Scheme Parameter	0.5
Propagation Step	1.55
Mesh: Number of Points	500
Boundary Conditions	PML
PML: Layers	6
PML: Theoretical Reflection Coefficient	1×10^{-6}

Figure 1 and Figure 2 show a typical MZI waveguide design with MZI symmetric and asymmetric structures, respectively. Single mode profile beam and 2D image of optical field propagation are also shown at the bottom of each of the design structures.

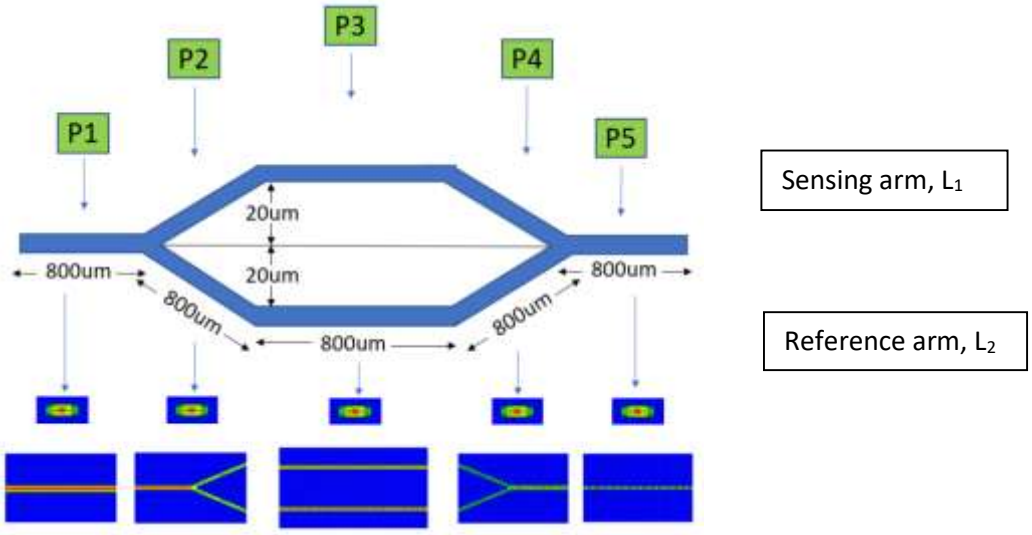

Figure 1. Waveguide design with MZI symmetrical structure.

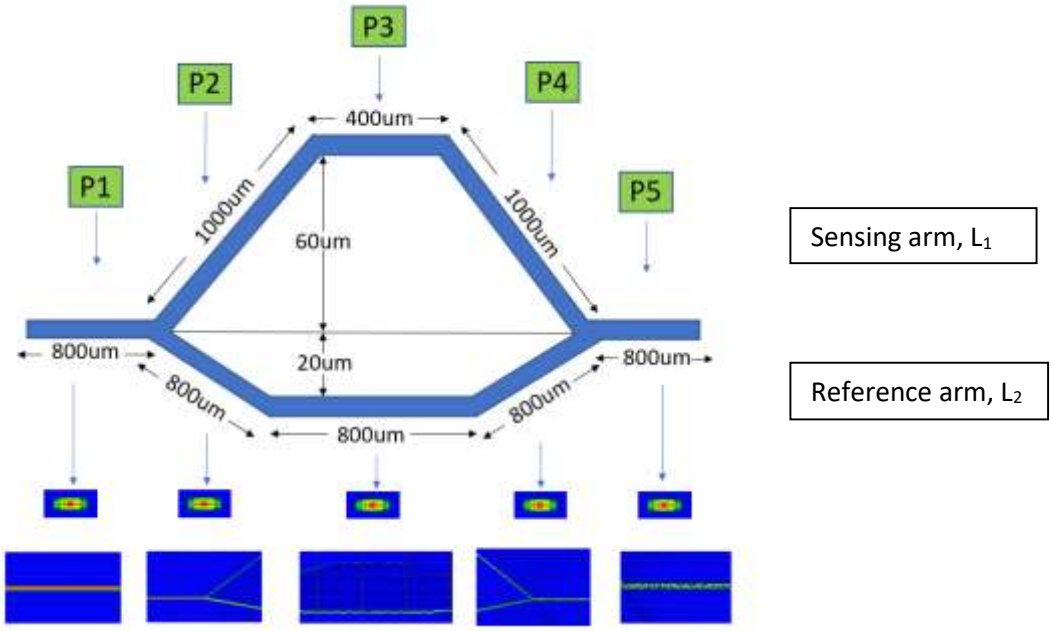

Figure 2. Waveguide design with MZI asymmetrical structure.

3. RESULTS AND DISCUSSION

Output power analysis was conducted at the main input and output of the waveguide and the overall results are shown in Figure 3 and Figure 4.

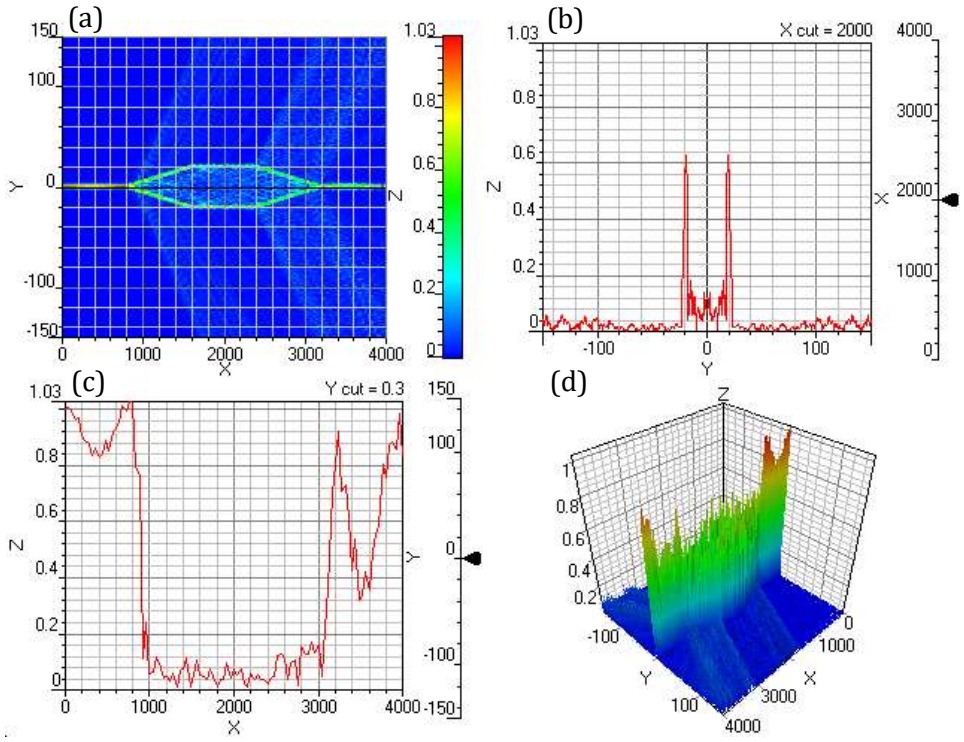

Figure 3. Measured power at various points (P1-P5) for MZI symmetrical design (a) first quadrant - optical field propagation in 2D view (b) second quadrant - the optical power distribution at the Z-Y axis (c) third quadrant -optical power distribution at Z-X axis and (d) fourth quadrant - optical field propagation in 3D view.

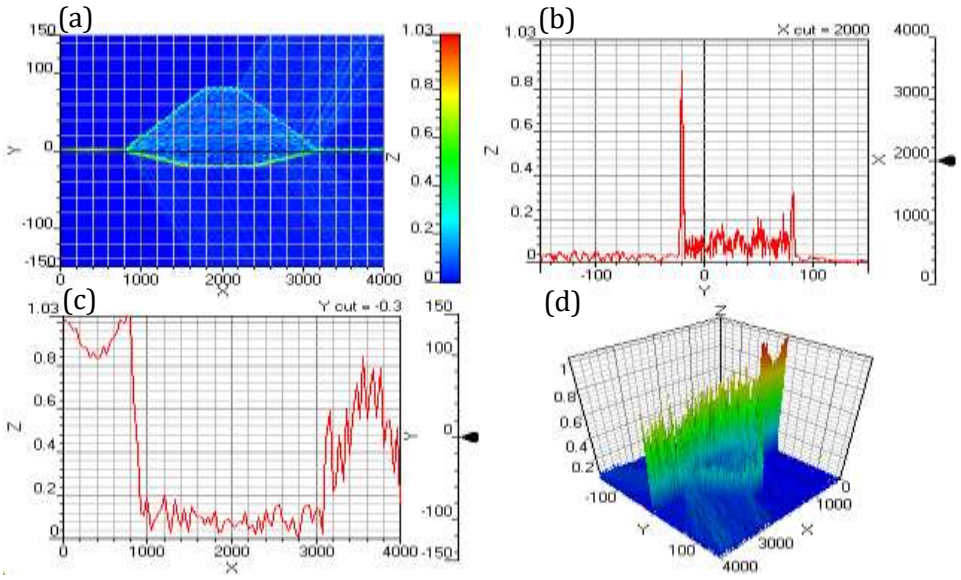

Figure 4. Measured power at various points (P1-P5) for MZI asymmetrical design.

All two designs produced similar patterns, especially in second and third quadrants. Before the light enters the sensing area, the power input is high. Later, there is a power drop within the sensing area. Consequently, the power is increased a bit higher when the light exits the sensing area. This is to show that there is a performance distribution of power throughout the waveguide. The power distribution trend of MZI asymmetrical design follow closely to that of the MZI symmetrical which suggest both designs worked properly. Table 3 lists all the measured power distribution at five main points throughout the structure which can be referred in Figure 1 and Figure 2. MZI symmetrical design has the highest output power among all, and this is probably due to less light splitting and recombining which leads to less power drop at the sensing arm [12]. As for MZI asymmetrical design, the output power is quite low compared to its symmetrical counterpart. This is probably due to when powers split to two MZI arms that are not in equal lengths resulting in degradation of the extinction ratio of the output interfering spectrum [13,14].

Table 3 2D simulation parameters

Design	P1	P2	P3	P4	P5
MZI symmetrical (sensing and reference arms)	1.00	0.66	0.70	0.62	0.90
MZI asymmetrical (sensing arm)	1.00	0.48	0.32	0.32	0.60
MZI asymmetrical (reference arm)	1.00	0.79	0.89	0.59	0.60

The comparison of Optical Field Propagation (OFP) for the two designs is also shown in Figure 5.

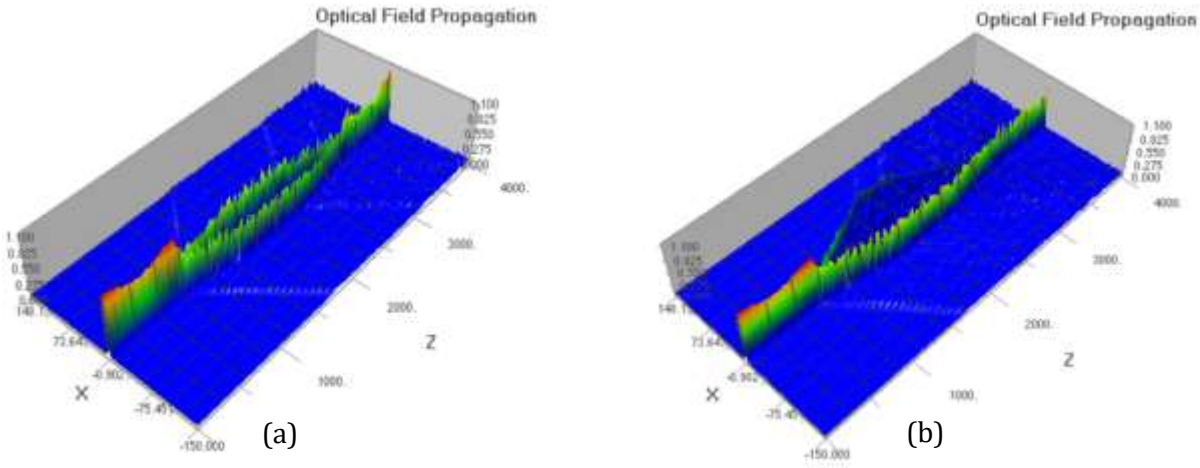

Figure 5. Optical Field Propagation (OFP) 3D view for (a) MZI symmetrical and (b) MZI asymmetrical.

Since the aim of this research is to obtain the highest output power with clear optical propagation path, hence only device size at 4000μm x 300μm is shown due to it yields higher output power among other sizes and have clear optical propagation path. A single mode profile with effective refractive index of 1.583 for both Transverse Electric (TE) and Transverse Magnetic (TM) fundamental modes was able to be obtained with the core layer dimension of 4μm width and 4μm height and effective refractive index (n_{eff}) versus waveguide core width (μm) are depicted in Figure 6 and Figure 7, respectively.

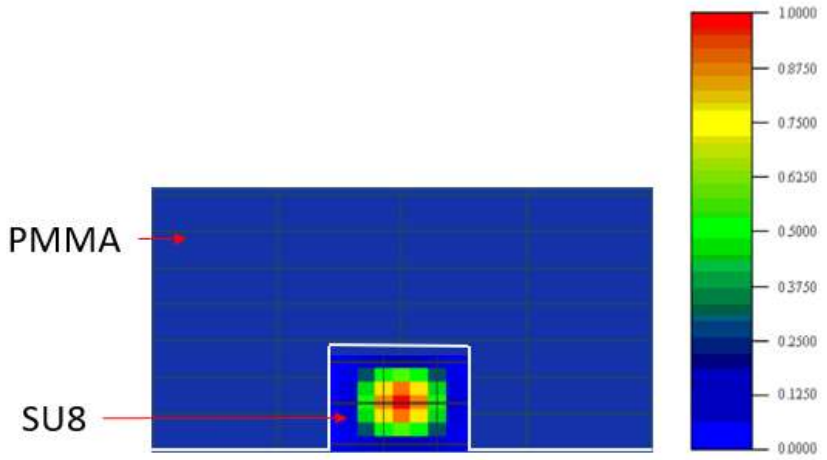

Figure 6. Single mode profile beam over the rectangular waveguide calculated from 3D beam propagation method (BPM) simulation.

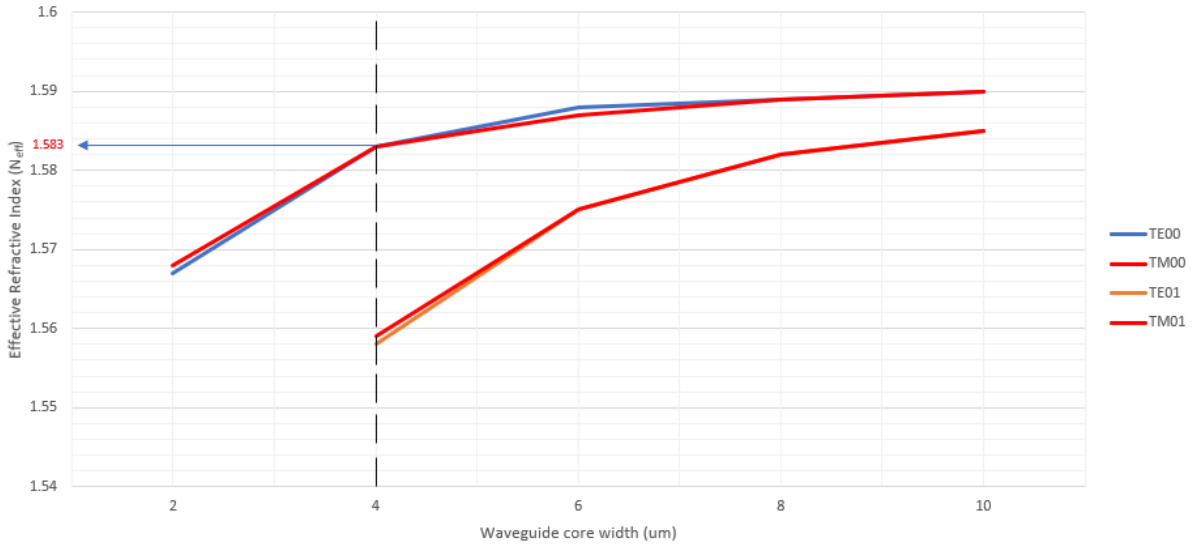

Figure 7. Effective refractive indices versus waveguide core width at 1550 nm wavelength.

4. CONCLUSION

Two MZI waveguide designs have been simulated and analyzed. The design with MZI symmetrical structure produced 0.90 a.u while its asymmetrical counterpart generated only 0.60 a.u output power. A waveguide that can produce a high output power with a clear optical propagation path is essential for a waveguide sensor to function properly, especially in having high sensitivity and good selectivity. Hence, a MZI waveguide having MZI symmetrical structure with a device size of 4000μm x 300μm fits the requirement effectively.

ACKNOWLEDGEMENTS

The authors would like to acknowledge the support from the Fundamental Research Grant Scheme (FRGS) under a grant number of 9003-00624/ FRGS/1/2017/STG02/UNIMAP/02/3 from the Ministry of Higher Education Malaysia.

REFERENCES

[1] N. Fabricius, G. Gauglitz and J. Ingenhoff, A gas sensor based on an integrated optical Mach-Zehnder interferometer, Elsevier Sequoia, Sensors and Actuators B, 7 (1992) 7672-676.

[2] Xiai Xia Ma, Kai Xin Chen et. al., Cost-Effective Mach-Zehnder Interferometer Liquid Refractive Index Sensor based on Conventional Polymer Strip Waveguide, IEEE Photonics Society, Vol. 13, No.1, (February 2021).

[3] Jiaqi Gong, Changyu Shen et. al., High sensitivity fiber temperature sensor based PDMS film on Mach-Zehnder interferometer, Elsevier, Optical Fiber Technology 53 (2019) 102029.

[4] Gengsong Li, Zhen Liu et al., Pb^{2+} fiber optic sensor based on smart hydrogel coated Mach-Zehnder interferometer, Elsevier, Optics and Laser Technology 145 (2022) 107453.

[5] Acacio Luiz Siarkowski, Leornado Frois Hernandez et al., Sensing based on Mach-Zehnder interferometer and hydrophobic thin films used on volatile organic compounds detection, SPIE, Optical Engineering 51 (5), 054401, (May 2021).

[6] Ning Zhao, Guang Qian et al., Integrated optical displacement sensor based on asymmetric Mach-Zehnder Interferometer Chip, SPIE, Optical Engineering 56(2), 027109 (February 2017).
[7] C.S Rizal and B. Niraula, Compact Si-based asymmetric MZI waveguide on SOI as a thermo-optical switch, Elsevier, Optics Communications, 0030-4018 (October 2017).
[8] Kyohei Okubo, Ken Uchiyamada et al., Silicon nitride directional coupler interferometer for surface sensing, SPIE, Optical Engineering, Vol. 56(1) 017101-1 (January 2017).
[9] Dr. Rudiger Paschotta, Mach Zehnder Interferometer, RP Photonics (2022), https://www.rp-photonics.com/interferometers.html.
[10] Lukas Chrostowski & Michael Hochberg, Silicon Photonics Design – From Devices to Systems, Cambridge University Press, First Edition, ISBN 978-1-107-08545-9, (2015).
[11] Prof. Robert G. Hunsperger, Losses in Optical Waveguides, Springer-Verlag Berlin Heidelberg, First Edition, ISBN 978-3-540-38843-2, (2002).
[12] Ana M. Gutierrez, Antoine Brimont et al., Method for measuring waveguide propagation losses by means of a Mach Zehnder Interferometer structure, Elsevier, Optics Communications 285 (2012) 1144-1147.
[13] Yiwei Xie, Ming Zhang et al., Design Rule of Mach-Zehnder Interferometer Sensors for Ultra-High Sensitivity, MDP, Sensors 20, 2640 (May 2020).
[14] Xiaoxia Ma, Jieyun Wu et al., On-chip integration of a metal-organic framework nanomaterial on a SiO_2 waveguide for sensitive VOC sensing, Royal Society of Chemistry, Lab on a Chip (August 2021).